Probing the Opening of the Pancreatic Lipase Lid Using Site-Directed Spin Labeling and EPR Spectroscopy

Valérie Belle,*,‡ André Fournel,*,‡ Mireille Woudstra,‡ Sébastien Ranaldi,‡ Florence Prieri,‡ Virginie Thomé,§ Julie Currault,§ Robert Verger,§ Bruno Guigliarelli,‡ and Frédéric Carrière*,§

Laboratoire de Bioénergétique et Ingénierie des Protéines, CNRS UPR 9036, IBSM, Marseille, France, and Laboratoire d'Enzymologie Interfaciale et de Physiologie de la Lipolyse, CNRS UPR 9025, IBSM, Marseille, France

Received August 8, 2006; Revised Manuscript Received December 20, 2006

ABSTRACT: Access to the active site of human pancreatic lipase (HPL) is controlled by a surface loop (the lid) that undergoes a conformational change in the presence of amphiphiles and lipid substrate. The question of how and when the lid opens still remains to be elucidated, however. A paramagnetic probe was covalently bound to the lid via the D249C mutation, and electron paramagnetic resonance (EPR) spectroscopy was used to monitor the conformational change in solution. Two EPR spectral components, corresponding to distinct mobilities of the probe, were attributed to the closed and open conformations of the HPL lid, based on experiments performed with the E600 inhibitor. The open conformation of the lid was observed in solution at supramicellar bile salt concentrations. Colipase alone did not induce lid opening but increased the relative proportions of the open conformation in the presence of bile salts. The opening of the lid was found to be a reversible process. Using various colipase to lipase molar ratios, a correlation between the proportion of the open conformation and the catalytic activity of HPL was observed.

X-ray crystallography studies on pancreatic lipase in the presence of various effectors have shown that this lipase has a two-domain structure, including a catalytic N-terminal domain with an α/β-hydrolase fold and a β-sandwich C-terminal domain (*1*−*3*). The active site in the N-terminal domain includes a Ser-His-Asp catalytic triad, and its access is controlled by a lid showing two different conformations (open and closed). The C-terminal domain is analogous to the C2 domains and is required for interactions with a lipid−water interface to occur (*4*). The C-terminal domain is also involved in interactions with colipase, a physiological cofactor required for the adsorption of the lipase at a lipid−water interface in the presence of competing amphiphiles such as bile salts (*5*). When the human pancreatic lipase−colipase complex was crystallized in the presence of bile salts and phospholipids, the lid adopted the open conformation, thus giving free access to the active site. The N-terminal part of colipase was also found to interact with the lid domain, thus forming a second lipase−colipase interaction site. On the basis of these structural findings, it was suggested that colipase may help to bring the catalytic N-terminal domain of pancreatic lipase into close contact with the lipid interface, where a drastic change occurs in the conformation of the lid.

The closed and open conformations of HPL[1] observed in the crystal structures are thought to correspond to the beginning and end of the opening of the lid, respectively. This complex process, which has also been observed in X-ray crystallography studies of other lipases (*6*−*9*), probably requires several steps and intermediate conformations of the lid, as observed with the lipase from *Thermomyces lanuginosus* (*10*). Although X-ray crystallography is a powerful technique, it mainly yields static information. How and when the lid opens is still a matter of discussion, although studies using lipase inhibitors (*11*), fluorescence spectroscopy (*12*), neutron diffraction (*13*), and small-angle neutron scattering (*14*) have indicated that the lid may be open in solution in the presence of bile salts and colipase. The presence of a lipid−water interface does not seem to be required to induce and stabilize the open conformation of the lid, exposing a large hydrophobic surface around the lipase active site. This open conformation can probably be stabilized in solution by interactions with bile salts or other detergent monomers, as suggested by the crystal structures of pancreatic lipases in which monomers of β-octyl glucoside (*15*) or tetraethylene glycol monooctyl ether (TGME) (*16*) were observed. The neutron diffraction study suggested that both bile salt micelles and colipase were required for induction of the open conformation of the lipase in solution via the formation of a ternary complex (*13*). Inhibition studies have shown, however, that the sole presence of bile salts suffices to induce a fast inactivation of pancreatic lipase, probably via the opening of the lid that normally prevents the access of inhibitors to the active site in solution (*17*). The various approaches used

* To whom correspondence should be addressed: Frédéric Carrière, Valérie Belle and André Fournel, IBSM, CNRS, 31 chemin Joseph Aiguier, 13402 Marseille cedex 20, France. Telephone: (33) 4 91 16 41 34. Fax: (33) 4 91 71 58 57. E-mail: carriere@ibsm.cnrs-mrs.fr.

‡ CNRS UPR 9036.

§ CNRS UPR 9025.

[1] Abbreviations: EPR, electron paramagnetic resonance; E600, diethyl *p*-nitrophenyl phosphate; HPL, human pancreatic lipase; MTSL, (1-oxyl-2,2,5,5-tetramethyl-Δ^3-pyrroline-3-methyl) methanethiosulfonate; NaTDC, sodium taurodeoxycholate; SDSL, site-directed spin labeling.

10.1021/bi0616089 CCC: $37.00
Published on Web 02/01/2007

Table 1: Primers Used for PCR Mutagenesis[a]

	primer sequences and comments
1	CCT GGA TCC GCT CGG CAT GCT, sense primer annealing to the HPL cDNA 5′ end, BamHI
2	CCA GGA TCC TCA GCA GGG TGT C, antisense primer annealing to the HPL cDNA 3′ end, BamHI
3	GCA GAA CCT T**A**C TTT CAG GGC, sense primer corresponding to the peptide AEP**Y**FQG and encoding the C181Y mutation
4	GCC CTG AAA G**T**A AGG TTC TGC, antisense primer corresponding to the peptide AEP**Y**FQG and encoding the C181Y mutation
5	TGT GGA CAT A**TG** CGG AAT CTG G, sense primer corresponding to the peptide VDI**C**GIW and encoding the D249C mutation
6	CCA GAT TCC G**CA** TAT GTC CAC A, antisense primer corresponding to the peptide VDI**C**GIW and encoding the D249C mutation

[a] Point mutations are shown in boldface type. Restriction sites are underlined.

up to now did not lend themselves to studying the opening process, the individual and/or synergistic effects of bile salts and colipase, or the possible coexistence of several lid conformations.

To further investigate the dynamic processes involved in the opening of the lid in pancreatic lipase, the use of spectroscopic techniques is required. Intrinsic tryptophan fluorescence has been used to monitor the conformational changes occurring in HPL interacting with the lipase inhibitor Orlistat in the presence of bile salts (*12*) or the interactions between *T. lanuginosus* lipase (TLL) and mixed micelles of *cis*-parinaric acid and bile salts (*18*). In both cases, it has been suggested that a tryptophan residue naturally present in the lid (W252 in HPL and W89 in TLL) is a good potential candidate for use as an internal probe. Although all the other tryptophan residues were mutated in TLL to increase the specificity of the fluorescence emission, the presence of seven tryptophan residues spread over the whole HPL structure made it difficult to interpret the changes in the pattern of fluorescence. Further studies with tryptophan mutants of HPL showed that the contribution of the solvent-exposed W30 residue to the overall fluorescence of wild-type HPL was much higher than that of the W252 located in the lid (*19*). To use W252 fluorescence to monitor the HPL lid opening process, it may therefore be necessary for of all the other tryptophan residues to be mutated. Fourier transform infrared attenuated total reflection (FTIR-ATR) methods have also been used to study the conformational changes and orientation of TLL occurring on a solid hydrophobic surface (*20*). Comparisons between the FTIR spectra obtained with TLL in solution and adsorbed on a hydrophobic surface mainly yielded information about the solvation of the protein. The use of deuterated buffer showed the occurrence of an unusual hydrogen−deuterium exchange in the peptide CONH groups of the adsorbed TLL molecules, which was consistent with the lipase being in the open conformation at the water−hydrophobic interface. No significant changes in the secondary structure of TLL were observed, however, upon adsorption, except for a slight folding of the β-structures as the lipase monolayer was formed. Therefore, the FTIR method does not seem to be a very sensitive method for studying the conformational changes occurring in a short helical peptide stretch such as the lid in large proteins such as lipases (the lid accounts for 23 residues of 449 in HPL).

In this study, electron paramagnetic resonance (EPR) spectroscopy combined with site-directed spin labeling (SDSL) was used to monitor the conformational changes occurring in the HPL lid in solution and to assess the effects of physiological partners of the lipase, i.e., colipase and bile salts. This technique has proven to be a powerful means of studying protein interactions and dynamic processes such as conformational changes (*21*−*23*). The SDSL strategy involves inserting a nitroxide radical into a selected site of a protein via a cysteine residue and observing its paramagnetic properties using EPR spectroscopy. When recorded at room temperature, the EPR spectrum reflects the mobility of the radical and thus provides information about its local environment. Any change in this environment resulting from either a physical or chemical event can then be identified from the change in the EPR signature.

EXPERIMENTAL PROCEDURES

DNA Source and Manipulations. The cDNA encoding HPL was previously obtained from human placenta mRNA using PCR technology (*24*). A 1411 bp BamHI DNA fragment containing the entire HPL coding region was subcloned into the pGAPZB *Pichia pastoris* transfer vector (Invitrogen), downstream of the GAP constitutive promoter. Plasmids were produced and amplified in *Escherichia coli* after electroporation of ElectroMAX DH10B cells (Life Technologies). Plasmid DNAs were isolated from *E. coli* cultures using the alkaline lysis procedure (*25*) and purified using the Wizard DNA purification system (Promega). Digestion with restriction enzymes and ligation with T4 DNA ligase were performed as recommended by the enzyme supplier (New England Biolabs). DNA sequencing was performed by Genome Express (Grenoble, France).

Site-Directed Mutagenesis. The HPL C181Y mutant was constructed using the PCR overlap extension technique (*26*) with internal oligonucleotides carrying the specific mutations, and two external oligonucleotides corresponding to the 5′ and 3′ ends of HPL cDNA, respectively. PCRs were carried out using *pfu* DNA polymerase (Stratagene). The first PCR was carried out using HPL cDNA in pGAPZB as the template and primers 1 and 4 (Table 1), for 30 cycles of 1 min at 94 °C, 2 min at 60 °C, and 3 min at 72 °C. The second PCR was carried out using HPL cDNA in pGAPZB as the template and primers 2 and 3 (Table 1), for 30 cycles of 1 min at 94 °C, 2 min at 60 °C, and 3 min at 72 °C. The third PCR ligation−amplification step was carried out using the products of PCR1 and PCR2 as the templates, and primers 1 and 2 for 30 cycles of 1 min at 94 °C, 2 min at 60 °C, and 3 min at 72 °C. The PCR3 product was digested with BamHI, and the resulting BamHI DNA fragment (1411 bp) containing the mutation was subcloned into the pGAPZB vector. Several clones were screened to check that the BamHI insert was properly oriented, and one of them was further sequenced to check that only the desired mutation was introduced by PCR. This clone (HPL C181Y mutant) was further used as a template for constructing the HPL C181Y/D249C double mutant. The additional D249C mutation was also introduced using the PCR overlap extension technique as described above, with primers 5 and 6 (Table 1) serving

as the internal oligonucleotides carrying the mutation. The final PCR product was digested with BamHI, and the resulting BamHI DNA fragment (1411 bp) containing the double mutation was subcloned into the pGAPZB vector. One clone in which the BamHI insert was correctly oriented was further sequenced.

Production of HPL and HPL Mutants in P. pastoris. Transformation of wild-type *P. pastoris* strain X-33 was performed by electroporation using a Bio-Rad gene pulser (1500 V, 200 Ω, 25 μF). Electrocompetent *P. pastoris* cells were prepared using standard methods (*27*). Prior to the yeast transformation procedure, the pGAPZB plasmid containing either HPL DNA or mutants was linearized with *Bsp*HI. *P. pastoris* cells were also transformed by the pGAPZB plasmid without any insert and used for negative control assays. The recombinant yeast clones were selected from the colonies growing on YPDS plates containing 100 μg/mL zeocin, after incubation for 3 days at 30 °C. The colonies were subsequently screened to identify HPL secreting transformants. In each construct, the best HPL activity-secreting clone was selected for the production of the recombinant protein. A preculture step was performed for 24 h in a 250 mL Erlenmeyer flask containing 50 mL of YPD medium. This preculture was further used to inoculate larger yeast cell cultures at an optical density (600 nm) of 1, to start the cell growth directly in the exponential growth phase, as well as to establish reproducible culture conditions. The yeast was further grown at 30 °C, with orbital agitation at a rate of 100 rpm. The cell cultures were usually performed in a 1 L Erlenmeyer flask containing 200 mL of YPD medium without any Zeocin, and the culture growth was stopped after 40 h to limit the proteolysis of the recombinant HPL (or mutant) secreted into the culture medium.

Purification of HPL and HPL Mutants. Two liters of yeast culture medium was collected, and the yeast was pelleted by centrifugation at 12 000 rpm for 15 min at 4 °C. After the pH was adjusted to 6.5, the culture supernatant was incubated for 1 h under batch conditions with S-Sepharose gel (sulfopropyl cation exchanger, Pharmacia) previously equilibrated in 10 mM MES buffer (pH 6.5). The incubation was performed at 4 °C under gentle stirring. More than 90% of the lipase activity was found to be bound to the gel when 20 mL of gel/L of culture supernatant was used. The gel was washed with twice its volume of 10 mM MES buffer (pH 6.5) and packed into a chromatographic column (IBF, 24 mm internal diameter) that was further connected to a FPLC device (Pharmacia). A linear NaCl gradient ranging from 0 to 0.2 M NaCl in 10 mM MES buffer (pH 6) was then applied for 1 h. The flow rate was adjusted to 1 mL/min. The protein elution profile was recorded spectrophotometrically at 280 nm, and 2 mL fractions were collected. The fractions containing HPL (or HPL mutant) were identified by measuring the lipase activity and performing SDS−PAGE. All fractions showing a major protein band at 50 kDa were pooled and concentrated.

Electrophoresis and Western Blotting Procedures. The recombinant HPL and HPL mutants present in the yeast culture medium and purification fractions were analyzed by electrophoresis on 12% polyacrylamide gels in the presence of SDS as described by Laemmli (*28*). Western Blotting was performed as described by Gershoni and Palade (*29*) using rabbit anti-HPL polyclonal antibodies diluted 1000 times. The reacting antibodies were detected with goat anti-rabbit immunoglobulins conjugated to alkaline phosphatase.

Analysis of Recombinant HPL and Mutants. Each production of HPL and HPL mutants was checked by performing amino acid analysis, N-terminal sequence analysis using an Applied Biosystem model 473A gas-phase sequencer to check that no proteolytic degradation had taken place, and MALDI-TOF mass spectrometry using Voyager DE-RP equipment (Perspective Biosystems Inc.). The stochiometry of accessible sulfhydryl groups (nonoxidized free cysteine) per lipase molecule was estimated from the titration with Elmann's reagent (*30*).

Spin Labeling Procedure. Since it was observed that free cysteines were oxidized in the recombinant lipase recovered from *Pichia* culture medium, the recombinant proteins were first reduced with DTT prior to the spin labeling reaction. HPL (8−10 mg/mL) was incubated with a 1000-fold molar excess of DTT for 30 min in ice. The excess DTT was then removed by performing gel filtration chromatography on a Superdex 75 column, using 10 mM MES, 150 mM NaCl buffer (pH 6.5). The fractions containing lipase activity were pooled and concentrated using 30 kDa cutoff polyethersulfone ultrafiltration membranes (Vivaspin 2, VivaSciences-Sartorius) to produce a lipase concentration of ∼8−10 mg/mL with a minimum loss of protein. The HPL was then labeled with (1-oxyl-2,2,5,5-tetramethyl-Δ^3-pyrroline-3-methyl) methanethiosulfonate (MTSL, Toronto Research Chemicals Inc., Toronto, ON) at a 10-fold molar excess, using a MTSL stock solution at 10 mg/mL in acetonitrile. The reaction was carried out for 1 h in ice, under gentle stirring and a continuous flow of nitrogen to prevent oxidation. The excess MTSL was then removed by performing a second gel filtration chromatography on a Superdex 75 column, using 10 mM MES, 150 mM NaCl buffer (pH 6.5). The fractions containing lipase activity were pooled and concentrated at ∼4 mg of HPL/mL (80 μM), as described above.

Lipase Activity Measurements Using a pHstat. HPL activity measurements were performed by measuring the amount of free fatty acids released from a mechanically stirred emulsion of tributyrin (TC4, puriss grade from Fluka) as described in ref *24*. Using a pHstat (TTT 80 Radiometer, Copenhagen, Denmark), the free fatty acids were automatically titrated with 0.1 N NaOH at a constant pH of 7.5. Each reaction was performed in a thermostated vessel (37 °C) containing 0.5 mL of TC4, 14.5 mL of 0.28 mM Tris-HCl buffer, 150 mM NaCl, 1.4 mM $CaCl_2$, and 0.5 mM sodium taurodeoxycholate (NaTDC). Recombinant HPL displays a maximum specific activity of 12 500 units/mg under these conditions. The lipolytic activities are expressed here in international units (U). One unit corresponds to 1 μmol of fatty acid released/min.

Covalent Inhibition of the Spin-Labeled HPL Lid Mutant by E600. The covalent inhibition of the spin-labeled HPL lid mutant by diethyl *p*-nitrophenylphosphate (E600) was monitored by measuring the residual lipase activity and recording the EPR spectra at various times. The experiments were performed in 10 mM MES buffer and 150 mM NaCl (pH 6.5) containing 40 μM spin-labeled HPL lid mutant and an E600 to lipase molar ratio of 100, as well as 4 mM NaTDC and 80 μM colipase when required. Each reaction was started by mixing 1 μL of a 110 mM E600 ethanolic

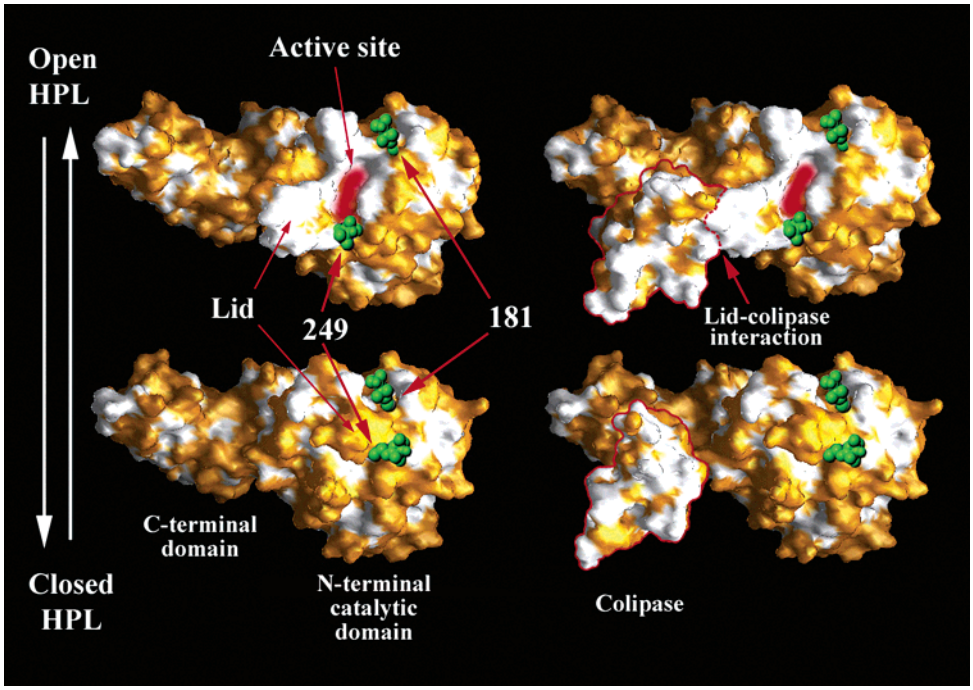

FIGURE 1: Molecular surface representation of HPL in its closed and open conformations, without and with colipase. Hydrophobic and polar surfaces are colored white and yellow, respectively. The sites selected for single spin labeling (C181 or D249C) are colored green (space-filling model).

solution with 27 μL of the protein solution incubated at 37 °C. Residual lipase activity was expressed as a function of the lipase activity measured in control samples without E600.

Reduction of Spin-Labeled HPL by DTT. The kinetics of the reduction of the spin-labeled HPL lid mutant by dithiothreitol (DTT) were monitored by recording EPR spectra at various times. The sample was prepared by mixing a solution of the spin-labeled C181Y/D249C HPL mutant (28 μL, 40 μM) with DTT (2 μL, 65 mM) at a molar excess of approximately 100-fold. The mixture was immediately transferred to a quartz capillary tube designed for EPR studies. This procedure allowed us to record the first EPR spectrum ~1 min after the addition of DTT, and the kinetics of the reaction were then observed for 1 h (acquisition time pro spectrum, 83 s). This experiment was repeated twice: without and with 4 mM NaTDC and colipase at a 2-fold molar excess versus HPL.

EPR Data Collection. EPR spectra were recorded at room temperature on an ESP 300E Bruker spectrometer equipped with an ELEXSYS Super High Sensitivity resonator operating at 9.9 GHz. Samples containing 40−80 μM spin-labeled HPL lid mutant were injected into a quartz capillary tube with a useful volume of ~20 μL. The microwave power was 10 mW, and the magnetic field modulation frequency and amplitude were 100 kHz and 0.1 mT, respectively. For the spin quantification, the double integration of the signal recorded under nonsaturating conditions was compared with that given by a standard $CuSO_4$ sample.

RESULTS

Spin Labeling of HPL and Effects on Lipase Kinetics. To select amino acid residues for site-directed spin labeling, the water accessible surface of HPL lid residues (C237-KKNILSQIVDIDGIWEGTRDFAA-C261) was estimated from the known "open" and "closed" three-dimensional structures of HPL, in the absence and presence of colipase. Some residues (W252, R256, and D257) are involved in the interaction with the HPL core, whereas others are involved in the interaction with colipase (N240, S243, and V246) when the lid is open. Among the 23 residues of the HPL lid, only residues D249, E253, and T255 had side chains which were fully exposed to solvent in both the open and closed conformations of the lid and were not involved in any interactions with the lipase core or the colipase. The D249 residue located in the lid was chosen as a target for spin labeling (Figure 1) and was replaced with a cysteine residue by perfoming site-directed mutagenesis. To ensure specific spin labeling at a single position, the other accessible free cysteines from HPL had to be mutated. HPL contains two well-characterized free cysteine residues at positions 103 and 181, but only C181 is accessible to sulfhydryl reagents such as dithionitrobenzoic acid (*30*, *31*). A tyrosine was substituted for C181 as observed at the equivalent position in other pancreatic lipases (*32*, *33*). The double C181Y/D249C HPL mutant was produced in the yeast *P. pastoris* and purified to homogeneity in a single cation exchange chromatography step, as described in Experimental Procedures.

Spin labeling was performed on the double D249C/C181Y HPL mutant as well as on the wild-type HPL containing the single accessible C181 using the procedure described in Experimental Procedures. In both cases, spin quantification (resulting in the concentration of paramagnetic centers) gave a labeling yield of ~80%, based on the known protein concentrations. Such a high yield of labeling was obtained only after the oxidized free cysteines were reduced via addition of a large excess of DTT (a 100−1000-fold molar excess vs lipase).

We verified that the HPL mutant, with and without spin labeling, had the same kinetic properties as HPL by measur-

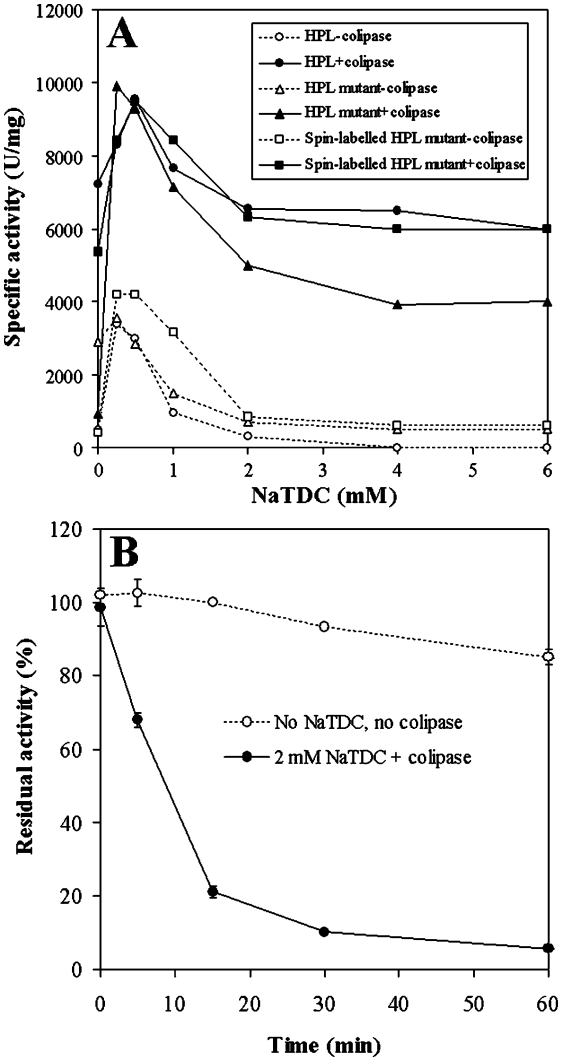

FIGURE 2: Kinetic properties of the spin-labeled HPL mutant. (A) Effects of bile salt concentration and colipase on the rate of tributyrin emulsion hydrolysis by HPL, the C181Y/D249C HPL mutant, and the spin-labeled HPL mutant. Specific activity is expressed in units per milligram of lipase, and 1 unit = 1 μmol of butyric acid released/min. Assays were performed in the absence (empty symbols) and presence (filled symbols) of a 2-fold molar excess of colipase. (B) Effects of E600 on the spin-labeled D249C HPL mutant in the absence and presence of bile salts and colipase.

ing its specific activity on tributyrin in the presence or absence of bile salts (NaTDC) and colipase (Figure 2A). The level of activity was similar to that recorded with HPL, whatever the conditions. Like HPL, the mutant was found (1) to be irreversibly denatured at the oil−water interface in the absence of bile salts and colipase, (2) to display maximum activity in the presence of 0.25−0.5 mM NaTDC, (3) to be inhibited by increasing bile salt concentrations above their critical micellar concentration (2 mM), and (4) to be reactivated by colipase. These properties were not affected by the covalent modification of C249 by the MTSL spin label reagent (Figure 2A). The inhibition of the spin-labeled C181Y/D249C HPL mutant by E600 was also investigated. Like HPL, the labeled mutant was inhibited by E600 only in the presence of micellar concentrations of bile salts, suggesting that the opening of the lid induced by bile salts and giving access to the active site in HPL was similar in both HPL and the spin-labeled HPL mutant (Figure 2B). These data showed that the mutation and labeling of HPL at such a crucial structural region for the catalytic mechanism, i.e., the lid, did not dramatically affect the kinetic behavior of the lipase, and it was thus possible to study the HPL activation process (the opening of the lid) using the spin-labeled HPL mutant and EPR spectroscopy.

EPR Spectra of Spin-Labeled HPL and HPL Mutant. The EPR spectrum of the nitroxide radical inserted into the HPL lid reflects the mobility of this probe through the averaging of both Zeeman and hyperfine interactions. Figure 3 (spectra 1−4) shows the spectral shapes observed in our study when the radical mobility varied. The spectrum of free MTSL (spectrum 1), reflecting a very high mobility of the radical, is given for comparison with the other spectral shapes. The spectrum of the C181Y/D249C HPL mutant labeled on the lid (spectrum 2) exhibited a relatively narrow single-component shape, with an outer line splitting of 3.22 (0.02) mT (Table 2), indicating a fairly fast motion of the radical typical of a solvent-exposed location (*34*). The spectrum of the HPL labeled at the level of C181 (spectrum 3) was drastically different and reflected a highly restricted nitroxide radical mobility, almost reaching the so-called "rigid-limit" regime (*35*) obtained for a frozen solution of MTSL (spectrum 4 and Table 2). This may be attributable to strong steric hindrance being exerted on the radical, since it was located at the bottom of a small surface pocket, as deduced from the location of C181 in the three-dimensional structure of HPL (Figure 1). We also recorded the EPR spectrum of the spin-labeled HPL mutant denatured by 1.5% SDS, and the spectral shape reflected an intermediate mobility in comparison with spectra 1 and 2 (data not shown). The radical in the denatured protein was therefore found to be more mobile than in the folded protein, as previously reported in the literature (*36*). Prior to the EPR measurement, the denaturation of the enzyme was checked by measuring the loss of enzyme activity.

Effects of Bile Salts and Colipase on the EPR Spectra. The effects of the physiological partners of HPL (colipase and/or bile salts) on the EPR spectral shapes of the spin-labeled HPL mutant are shown in Figure 3 (spectra 5−8). The presence of colipase at a colipase to lipase molar ratio of 2 (spectrum 5) did not induce any change in the EPR spectrum, which was identical to spectrum 2 recorded with the spin-labeled HPL mutant alone in solution, with an outer line splitting of 3.22 ± 0.02 mT. When bile salts at a concentration of 4 mM were added to a solution containing the spin-labeled HPL mutant, the spectrum became composite with two components exhibiting different mobilities of the nitroxide radical (spectrum 6). The relatively narrow spectral shape with an outer line splitting of 3.22 ± 0.02 mT (arrows with ○ and Table 2) corresponded to spectrum 2 obtained with the spin-labeled HPL mutant alone in solution. This shape will here be called the fast-motion component. The second component had a very broad spectral shape (arrows with ∗), reflecting a highly restricted mobility of the radical as indicated by its outer line splitting of 6.65 ± 0.05 mT (Table 2). This shape will here be called the slow-motion component. When both physiological partners were present, the proportion of the slow-motion component increased strongly (spectrum 7). To isolate this particular component, we subtracted the fast-motion component (spectrum 2) from the composite spectrum (spectrum 7). The subtraction was performed manually with the criterion of cancelling the high-

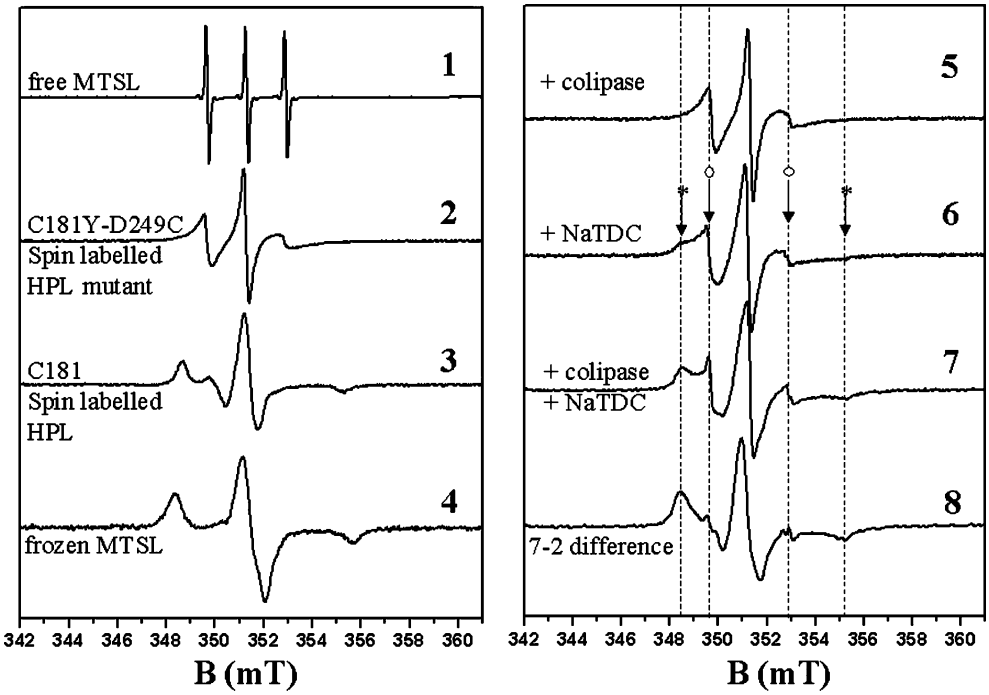

FIGURE 3: EPR spectra of spin-labeled HPL and HPL mutant. Effects of bile salts and colipase: (left) free MTSL in solution (spectrum 1), spin-labeled D249C/C181Y HPL mutant (spectrum 2), HPL labeled on the natural cysteine 181 (spectrum 3), and frozen solution of MTSL (spectrum 4) and (right) spin-labeled HPL mutant with colipase (spectrum 5), spin-labeled HPL mutant with 4 mM NaTDC (spectrum 6), spin-labeled HPL mutant with colipase and 4 mM NaTDC (spectrum 7), and the difference spectrum obtained by subtracting spectrum 2 from the composite spectrum 7 (spectrum 8). The arrows with asterisks indicate the positions of the low- and high-field lines of the slow-motion component and the arrows with circles those of the fast-motion component. EPR spectra 1−3 and 5−8 were recorded at room temperature and 9.9 GHz with a microwave power of 10 mW and a magnetic field modulation frequency and amplitude of 100 kHz and 0.1 mT, respectively. Spectrum 4 of the frozen solution of MTSL was recorded at 9.4 GHz and 200 K with a microwave power of 4 mW and a magnetic field modulation frequency and amplitude of 100 kHz and 0.3 mT, respectively.

Table 2: Outer Line Splittings Measured from EPR Spectra

sample	outer line splitting (mT)
spin-labeled C181Y/ D249C HPL mutant	
fast-motion component	3.22 ± 0.02
slow-motion component	6.65 ± 0.05
C181 spin-labeled HPL	6.53 ± 0.05
frozen MTSL	7.25 ± 0.05

field spectral line of the fast-motion component centered at around 353 mT. It should be noted that a residual contribution of a radical with high mobility was still present after subtraction, but this contribution was less than 1−2% of the total spin-labeled protein and was attributed to very low levels of either spin-labeled denatured proteins or protein fragments in our samples. The result of this subtraction was spectrum 8, which had a shape comparable to that obtained with HPL labeled at position 181 (spectrum 3) but slightly different, however, with respect to the outer line splitting (Table 2). This particular shape of the spectrum is representative of a radical located at a site poorly accessible to solvent (*34*). To quantitate the respective contributions of both components, composite spectrum 7 (total integrated intensity, I_{tot}) and spectrum 8 (I_{sm}) resulting from the subtraction were integrated separately and the proportion of the slow-motion component was deduced from I_{sm}/I_{tot}. As a control, we checked that the addition of the same amounts of colipase and/or bile salts to HPL labeled at position 181 did not induce any change in the EPR spectrum (data not shown), with a similar outer line splitting of 6.53 ± 0.05 mT (Table 2).

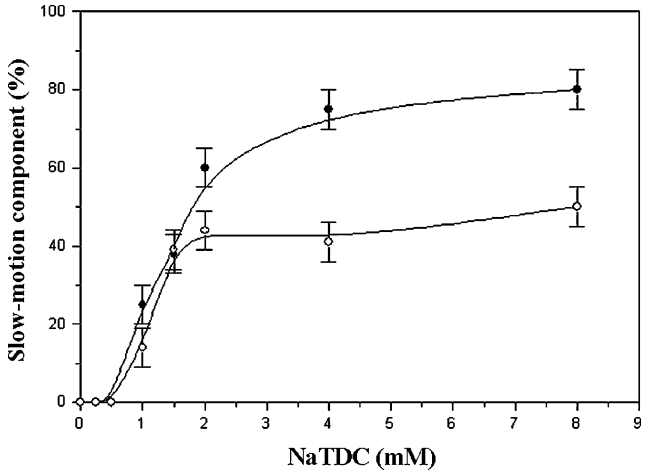

FIGURE 4: Changes in the proportion of the EPR spectrum slow-motion component of the spin-labeled HPL mutant with the NaTDC concentration: (○) experiments performed without colipase and (●) experiments performed with a 2/1 colipase/lipase molar ratio. The standard deviation of the relative proportions of the slow-motion component, due to both errors of subtraction and integrated intensity measurements, was estimated to be ±8%.

To further monitor the changes in the two components, the effects of the bile salt concentration on the spectral shapes were studied by recording the EPR spectra of the spin-labeled HPL mutant in solution, in either the absence or presence of colipase at a colipase to lipase molar ratio of 2 (Figure 4). Up to 0.5 mM NaTDC and in the absence of colipase, the shape of the EPR spectrum remained the same as that observed without bile salts and colipase (data not shown), which suggests that the radical was still in the same local

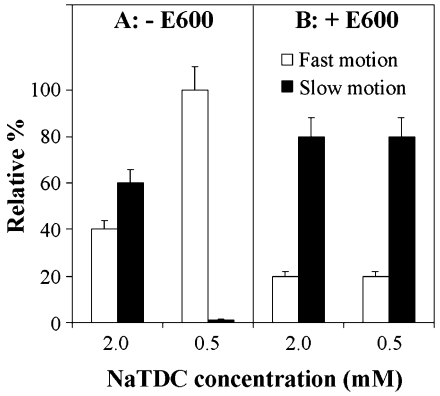

FIGURE 5: Dilution experiments showing the effects of bile salt concentration and E600 on the EPR spectral components. The bile salt concentration was reduced from 2 to 0.5 mM NaTDC by diluting the samples of spin-labeled HPL mutant in the absence (A) and presence (B) of E600 at a 1/100 lipase/inhibitor molar ratio. These experiments were performed in the presence of colipase at a 2/1 colipase/lipase molar ratio.

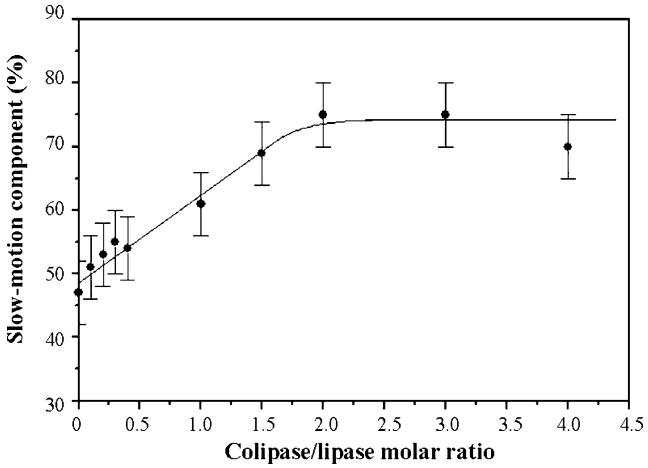

FIGURE 6: Changes in the EPR spectrum slow-motion component of the spin-labeled HPL mutant with the colipase/lipase molar ratio. All experiments were performed with 4 mM NaTDC. The standard deviation of the relative proportions of the slow-motion component proportion, due to both errors of subtraction and integrated intensity measurements, was estimated to be ±8%.

environment. Above 1 mM NaTDC, the proportion of the slow-motion component quickly increased with NaTDC concentration and reached a plateau at 40−50% in the absence of colipase and 80% in its presence. We determined whether this process was reversible by performing an experiment in which the bile salt concentration was reduced from 2 to 0.5 mM by dilution of the sample. The proportion of the EPR spectrum slow-motion component was found to decrease from 60 to 0% (Figure 5A).

The effects of the colipase/lipase molar ratio were investigated by recording the EPR spectra of the spin-labeled HPL mutant in a solution containing 4 mM NaTDC with variable amounts of colipase (Figure 6). Without colipase, the proportion of the slow-motion component spectrum corresponded to 45% of the total labeled proteins. This proportion gradually increased with increasing amounts of colipase and reached a maximum of 70−75% above a colipase to lipase molar ratio of 2.

Covalent Inhibition of the Spin-Labeled HPL Mutant by E600. After the covalent inhibitor E600 had been added to a spin-labeled HPL mutant solution, the residual activity with

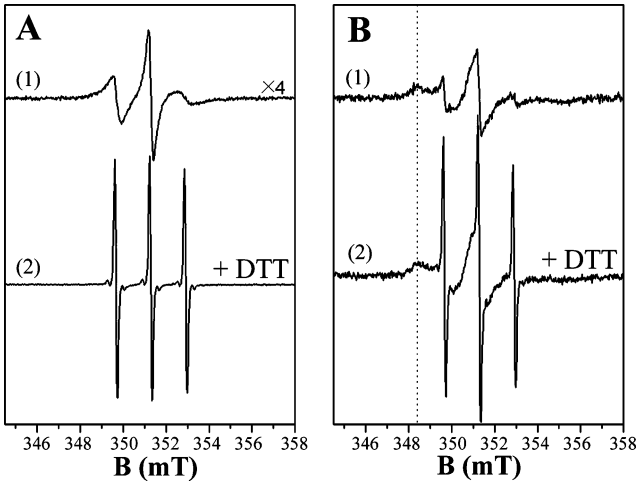

FIGURE 7: Reduction of the spin-labeled C181Y/D249C HPL mutant by DTT. (A) Spin-labeled D249C/C181Y HPL mutant (40 μM) before (1) and after (2) the addition of DTT. Spectrum 1 was magnified by a factor 4 to allow its comparison with spectrum 2. (B) Spin-labeled D249C/C181Y HPL mutant (40 μM) with colipase and 4 mM NaTDC before (1) and after (2) the addition of DTT. The dotted line indicates the low-field line of the slow-motion component of the EPR spectrum. EPR spectra were recorded with a microwave power of 10 mW and a magnetic field modulation frequency and amplitude of 100 kHz and 0.1 mT, respectively. Four scans were carried out to increase the signal-to-noise ratio, and the total acquisition time was 6 min.

time was measured simultaneously with the recording of the EPR spectra. We checked that in the absence of colipase and bile salts, the rate of lipase inhibition by E600 was extremely slow, and 85 ± 6% residual activity measured after incubation for 60 min (Figure 2B). Under these conditions, the EPR spectrum remained mainly composed of a fast-motion component (data not shown). When the experiments were performed in the presence of micellar concentrations of NaTDC (2−4 mM) and colipase, the inhibition rate increased significantly, showing a half-time of ∼8−9 min (Figure 2B). After incubation for 15 min with E600 (79 ± 2% HPL inhibition), the EPR spectrum was mainly composed of a slow-motion component (80%, Figure 5B). When the bile salt concentration was reduced from 2 to 0.5 mM by dilution, the EPR spectrum remained unchanged (Figure 5B), which suggests that the presence of E600 covalently linked to the active serine of HPL impaired the reversible closing of the lid.

Reduction of the Spin-Labeled HPL Lid Mutant by DTT. The kinetics of reduction of the spin-labeled C181Y/D249C HPL mutant by an excess of DTT were monitored by EPR spectroscopy in the absence (Figure 7A) and presence (Figure 7B) of 4 mM NaTDC and colipase. For each experiment, spectra 1 and 2 were acquired before and after the addition of DTT, respectively, the latter accumulating during the first 6 min of the reaction (four scans). Whatever the experimental conditions, the fast-motion component of the EPR spectrum of the spin-labeled HPL was found to disappear immediately after addition of DTT, and it was totally converted into a signal of an unbound, free-rotating radical in solution (Figure 7A,B). On the other hand, the slow-motion component of the EPR spectrum obtained in the presence of bile salts and colipase remained unchanged (Figure 7B) up to 30 min after the reduction reaction was started.

DISCUSSION

The aim of this study was to use EPR spectroscopic methods to observe the conformational changes in the HPL lid previously identified in X-ray crystallography studies (*1*−*3*, *16*). SDSL was performed to introduce a nitroxide radical at position 249 in the lid peptide stretch, and its mobility, as reflected by the EPR spectrum, was investigated under various conditions. The idea was to associate EPR spectra with various conformations of the HPL lid. The EPR spectrum was found to be composed of two components reflecting a slow and a fast motion of the radical (Figure 3). In the presence of micellar bile salt concentrations, the proportion of the slow-motion component increased significantly and was taken to be associated with the open conformation of the lid. This change in the EPR spectrum might, however, result from a conformational alteration not correlated with a motion of the lid. To unambiguously confirm the association between a given EPR spectrum component and a well-defined conformation, we used the E600 inhibitor to block the HPL lid in its open conformation since the X-ray crystallography findings showed that the HPL lid is open when an inhibitor is covalently linked to the active site serine. Since the covalent inhibition of HPL induced by E600 is irreversible, it is impossible for the lid to return to its closed conformation, mainly because this would require another conformational change in the β5 loop, and this change is impossible because residues from the β5 loop are involved in the oxyanion hole. When the bile salt concentration was reduced, no decrease in the proportion of the EPR spectrum slow-motion component was observed in the presence of E600, whereas the slow-motion component disappeared in the absence of E600 (Figure 5). The slow-motion component of the EPR spectrum can therefore be attributed to the open conformation of the HPL lid. In the absence of bile salts, the spin-labeled HPL mutant is not inhibited by E600, i.e., the active site is not accessible, and the EPR spectrum definitely reflects a fast motion of the radical. From this finding, the fast-motion component of the EPR spectrum is now attributable to the closed conformation of the HPL lid.

The shape of the slow-motion EPR spectrum component was found to be characteristic of a nitroxide being in the slow-motion regime, typical of radicals located at buried sites either within the compact hydrophobic core of a protein (*34*) or in proteins embedded in membrane lipids (*37*, *38*). A similar spectral shape was observed with the labeled wild-type HPL (Figure 3, spectrum 3) where the radical is covalently linked to residue C181 located at the bottom of a surface pocket. Its mobility is restrained by the tight packing of the amino acid residues surrounding this pocket as observed from a three-dimensional molecular model (data not shown). For the HPL lid mutant, the fact that the nitoxide radical at position 249 had a reduced mobility in the open conformation of the lid was unexpected since residue 249 was chosen for the high accessibility to solvent of its side chain in both the open and closed conformations of the lid (Figure 1). From the crystal structures of HPL, the *B*-factors (thermic agitation) of the side chain atoms of residue D249 were found to be similar in both the open (58.1 ± 4.8) and closed (62.7 ± 2.3) conformations of the HPL lid, and they suggested a high mobility of the D249 side chain in both conformations. It is worth noticing, however, that the open lid is not expected to be more mobile than the closed lid, because it is stabilized by several interactions with the HPL core (salt bridge, H-bonds), as well as with colipase (Figure 1). One possible explanation for the reduced mobility of the radical in the open lid is the fact that bile salt molecules could bind the HPL in its open conformation, in the vicinity of the radical, and thus restrain its mobility. The existence of a bile salt molecule in the vicinity of the active site of bile salt-stimulated lipase has already been reported in the literature (*39*). Another possible explanation could be that HPL monomers interact via their hydrophobic surfaces generated upon lid opening. A quaternary structure of this kind was observed in the crystal structure of the open HPL (*15*). Some of the detergent molecules (β-octyl glucoside), needed for the crystallization, were also observed in the crystal within the surface of interaction of the HPL monomers. Some of them were located at the entrance of the active site, bound to the hydrophobic part of the lid (*15*). In this case, the environment of residue 249 is severely restricted and one can assume that a radical present at this position will exhibit a highly restricted mobility. To check the solvent accessibility of residue 249, we monitored by EPR spectroscopy the reduction of the spin-labeled HPL lid mutant by DTT. These experiments showed qualitatively that the population of spin labels giving the slow-motion component was much less sensitive to DTT than the one giving the fast-motion component. These results suggest a lower solvent accessibility of residue 249 in the open conformation of the HPL lid, and they are in good agreement with the mobility analysis.

The ratio between the slow- and fast-motion components of the EPR spectrum was further used to investigate the effects of colipase and bile salts on the lid opening in solution. In the absence of bile salts, adding colipase did not induce the opening of the lid. Colipase can therefore only interact with the C-terminal domain of HPL, and this finding is consistent with the low affinity of lipase for colipase (1−2 μM^{-1}) measured in solution in the absence of lipids and amphiphiles (*40*, *41*). When colipase was added in the presence of micellar bile salt concentrations (4 mM NaTDC), a further increase in the proportion of the slow-motion EPR spectrum component was observed in comparison with the effects of bile salts alone. This result suggests that the open lid conformation is stabilized by colipase, probably as the result of the secondary interaction observed in X-ray crystallography studies between colipase and the lid (*3*), as well as the fact that the apparent affinity of lipase for colipase is increased by several orders of magnitude in the presence of bile salts or other amphiphiles [2×10^7−10^9 M^{-1} (*42*−*44*)].

We established here that the open and closed conformations of the lid are in equilibrium in the presence of bile salts. This equilibrium can be shifted either toward the lid opening (corresponding to the EPR spectrum slow-motion component) with an increase in bile salt concentration and addition of colipase or toward the closed conformation via dilution of the solution to decrease the bile salt concentration below the CMC. The proportion of the open conformation increases with the colipase to lipase molar ratio, reaching a maximum opening rate at a 2/1 ratio. This ratio is identical to that required for measuring maximum HPL activity on

triglyceride emulsions in the presence of bile salts (*5*). The changes in HPL activity observed with increasing amounts of colipase therefore seem to be linked to the opening of the lid.

Under all the experimental conditions that were used, 100% of the open conformation was never observed in solution, in contrast to what was observed in the crystal structure of the open HPL (*3*, *15*). Phospholipids, bile salts, other detergents, and a hydrophobic inhibitor were, however, required to crystallize HPL in its open conformation. In a liquid phase, the presence of lipid substrate and the resulting oil−water interface are probably required to shift the conformational equilibrium toward the full opening of the lid.

This study shows that SDLS combined with EPR spectroscopy provides a powerful technique for studying the HPL lid opening process in solution. This method can be used to nonambiguously attribute specific EPR spectral components to the closed and open conformations previously identified by X-ray crystallography. We now have an efficient tool for investigating the lid opening under various conditions, in isotropic solutions as well as in the presence of lipid aggregates. This tool might be particularly helpful for answering one of the remaining questions in the field of lipase enzymology: Is the lid opening ("structural activation") related to the kinetic phenomenon of "interfacial activation" of lipases (*45*, *46*), i.e., the drastic increase in enzyme activity observed with partly soluble triglyceride substrates (tripropionin) at a concentration above the solubility limit? This has not been demonstrated up to now, although it is quite common to read that the open structures of lipases reveal how these enzymes are activated at lipid interfaces. Another field of investigation opened by SDSL of the HPL lid is the structural behavior of the lipase in organic solvents or a biphasic environment. Lipases are commonly used as enantioselective biocatalysts under these conditions, but no structural information about the enzyme in such an environment is available. It has been proposed that the low reaction rates often observed might result from the partial lipase denaturation in the presence of solvent, as well as from a low level of lid opening. Several studies were performed to stabilize the open conformation of the lipase lid in the presence of organic solvents (*47*, *48*), but structural data are still missing.

ACKNOWLEDGMENT

We are grateful to Régine Lebrun and Danièle Monier for carrying out the N-terminal sequencing and MALDI-TOF mass spectrometry of the HPL C181Y/D249C mutant. We thank Mrs. Jessica Blanc for revising the English manuscript.

REFERENCES

1. Winkler, F. K., d'Arcy, A., and Hunziker, W. (1990) Structure of human pancreatic lipase, *Nature 343*, 771−774.
2. van Tilbeurgh, H., Sarda, L., Verger, R., and Cambillau, C. (1992) Structure of the pancreatic lipase-procolipase complex, *Nature 359*, 159−162.
3. van Tilbeurgh, H., Egloff, M.-P., Martinez, C., Rugani, N., Verger, R., and Cambillau, C. (1993) Interfacial activation of the lipase-procolipase complex by mixed micelles revealed by X-ray crystallography, *Nature 362*, 814−820.
4. Chahinian, H., Bezzine, S., Ferrato, F., Ivanova, M. G., Perez, B., Lowe, M. E., and Carriere, F. (2002) The β 5′ loop of the pancreatic lipase C2-like domain plays a critical role in the lipase-lipid interactions, *Biochemistry 41*, 13725−13735.
5. Bezzine, S., Ferrato, F., Ivanova, M. G., Lopez, V., Verger, R., and Carriere, F. (1999) Human pancreatic lipase: Colipase dependence and interfacial binding of lid domain mutants, *Biochemistry 38*, 5499−5510.
6. Brzozowski, A. M., Derewenda, U., Derewenda, Z. S., Dodson, G. G., Lawson, D. M., Turkenburg, J. P., Bjorkling, F., Huge-Jensen, B., Patkar, S. A., and Thim, L. (1991) A model for interfacial activation in lipases from the structure of a fungal lipase-inhibitor complex, *Nature 351*, 491−494.
7. Grochulski, P., Li, Y., Schrag, J. D., Bouthillier, F., Smith, P., Harrison, D., Rubin, B., and Cygler, M. (1993) Insights into interfacial activation from an open structure of *Candida rugosa* lipase, *J. Biol. Chem. 268*, 12843−12847.
8. Grochulski, P., Li, Y., Schrag, J. D., and Cygler, M. (1994) Two conformational states of *Candida rugosa* lipase, *Protein Sci. 3*, 82−91.
9. Roussel, A., Miled, N., Berti-Dupuis, L., Riviere, M., Spinelli, S., Berna, P., Gruber, V., Verger, R., and Cambillau, C. (2002) Crystal structure of the open form of dog gastric lipase in complex with a phosphonate inhibitor, *J. Biol. Chem. 277*, 2266−2274.
10. Brzozowski, A. M., Savage, H., Verma, C. S., Turkenburg, J. P., Lawson, D. M., Svendsen, A., and Patkar, S. (2000) Structural origins of the interfacial activation in *Thermomyces* (*Humicola*) *lanuginosa* lipase, *Biochemistry 39*, 15071−15082.
11. Rouard, M., Sari, H., Nurit, S., Entressangles, B., and Desnuelle, P. (1978) Inhibition of pancreatic lipase by mixed micelles of diethyl p-nitrophenyl phosphate and the bile salts, *Biochim. Biophys. Acta 530*, 227−235.
12. Lüthi-Peng, Q., and Winkler, F. K. (1992) Large spectral changes accompany the conformational transition of human pancreatic lipase induced by acylation with the inhibitor tetrahydrolipstatin, *Eur. J. Biochem. 205*, 383−390.
13. Hermoso, J., Pignol, D., Penel, S., Roth, M., Chapus, C., and Fontecilla-Camps, J. C. (1997) Neutron crystallographic evidence of lipase-colipase complex activation by a micelle, *EMBO J. 16*, 5531−5536.
14. Pignol, D., Ayvazian, L., Kerfelec, B., Timmins, P., Crenon, I., Hermoso, J., Fontecilla-Camps, J. C., and Chapus, C. (2000) Critical role of micelles in pancreatic lipase activation revealed by small angle neutron scattering, *J. Biol. Chem. 275*, 4220−4224.
15. Egloff, M.-P., Marguet, F., Buono, G., Verger, R., Cambillau, C., and van Tilbeurgh, H. (1995) The 2.46 Å resolution structure of the pancreatic lipase-colipase complex inhibited by a C_{11} alkyl phosphonate, *Biochemistry 34*, 2751−2762.
16. Hermoso, J., Pignol, D., Kerfelec, B., Crenon, I., Chapus, C., and Fontecilla-Camps, J. C. (1996) Lipase activation by nonionic detergents. The crystal structure of the porcine lipase-colipase-tetraethylene glycol monooctyl ether complex, *J. Biol. Chem. 271*, 18007−18016.
17. Moreau, H., Moulin, A., Gargouri, Y., Noël, J.-P., and Verger, R. (1991) Inactivation of gastric and pancreatic lipases by diethyl p-nitrophenyl phosphate, *Biochemistry 30*, 1037−1041.
18. Yapoudjian, S., Ivanova, M. G., Brzozowski, A. M., Patkar, S. A., Vind, J., Svendsen, A., and Verger, R. (2002) Binding of *Thermomyces* (*Humicola*) *lanuginosa* lipase to the mixed micelles of cis-parinaric acid/NaTDC, *Eur. J. Biochem. 269*, 1613−1621.
19. Ramos, P., Coste, T., Piemont, E., Lessinger, J. M., Bousquet, J. A., Chapus, C., Kerfelec, B., Ferard, G., and Mely, Y. (2003) Time-resolved fluorescence allows selective monitoring of Trp30 environmental changes in the seven-Trp-containing human pancreatic lipase, *Biochemistry 42*, 12488−12496.
20. Noinville, S., Revault, M., Baron, M. H., Tiss, A., Yapoudjian, S., Ivanova, M., and Verger, R. (2002) Conformational changes and orientation of *Humicola lanuginosa* lipase on a solid hydrophobic surface: An in situ interface Fourier transform infrared-attenuated total reflection study, *Biophys. J. 82*, 2709−2719.
21. Columbus, L., and Hubbell, W. L. (2002) A new spin on protein dynamics, *Trends Biochem. Sci. 27*, 288−295.
22. Hubbell, W. L., Cafiso, D. S., and Altenbach, C. (2000) Identifying conformational changes with site-directed spin labeling, *Nat. Struct. Biol. 7*, 735−739.
23. Biswas, R., Kuhne, H., Brudvig, G. W., and Gopalan, V. (2001) Use of EPR spectroscopy to study macromolecular structure and function, *Sci. Prog. 84*, 45−67.

24. Thirstrup, K., Carrière, F., Hjorth, S., Rasmussen, P. B., Wöldike, H., Nielsen, P. F., and Thim, L. (1993) One-step purification and characterization of human pancreatic lipase expressed in insect cells, *FEBS Lett. 327*, 79−84.
25. Sambrook, J., Fritsch, E. F., and Maniatis, T. (1989) *Molecular cloning. A laboratoty manual*, 2nd ed., Cold Spring Harbor Laboratory Press, Plainview, NY.
26. Higuchi, R. (1992) Using PCR to engineer DNA, in *PCR Technology: Principles and Applications for DNA Amplification* (Erlich, H. A., Ed.) pp 61−70, W. H. Freeman and Co., New York.
27. Cregg, J. M., and Russell, K. A. (1998) Transformation Methods, *Mol. Biol. 103*, 27−39.
28. Laemmli, U. K. (1970) Cleavage of structural proteins during the assembly of the head of bacteriophage T4, *Nature 227*, 680−685.
29. Gershoni, J. M., and Palade, G. E. (1982) Electrophoretic transfer of proteins from sodium dodecyl sulfate-polyacrylamide gels to a positively charged membrane filter, *Anal. Biochem. 124*, 396−405.
30. Verger, R., Sarda, L., and Desnuelle, P. (1970) The sulfhydryl groups of pancreatic lipase, *Biochim. Biophys. Acta 207*, 377−379.
31. Cudrey, C., van Tilbeurgh, H., Gargouri, Y., and Verger, R. (1993) Inactivation of pancreatic lipases by amphiphilic reagents 5-(dodecyldithio)-2-nitrobenzoic acid and tetrahydrolipstatin. Dependence upon partitioning between micellar and oil phases, *Biochemistry 32*, 13800−13808.
32. Hjorth, A., Carrière, F., Cudrey, C., Wöldike, H., Boel, E., Lawson, D. M., Ferrato, F., Cambillau, C., Dodson, G. G., Thim, L., and Verger, R. (1993) A structural domain (the lid) found in pancreatic lipases is absent in the guinea pig (phospho)lipase, *Biochemistry 32*, 4702−4707.
33. Carrière, F., Thirstrup, K., Hjorth, S., and Boel, E. (1994) Cloning of the classical guinea pig pancreatic lipase and comparison with the lipase related protein 2, *FEBS Lett. 338*, 63−68.
34. Mchaourab, H. S., Lietzow, M. A., Hideg, K., and Hubbell, W. L. (1996) Motion of spin-labeled side chains in T4 lysozyme. Correlation with protein structure and dynamics, *Biochemistry 35*, 7692−7704.
35. Marsh, D. (1989) Spin Labeling, in *Biological Magnetic Resonance* (Berliner, L. J., and Reuben, J., Eds.) pp 255−300, Plenum Press, New York.
36. Qu, K., Vaughn, J. L., Sienkiewicz, A., Scholes, C. P., and Fetrow, J. S. (1997) Kinetics and motional dynamics of spin-labeled yeast iso-1-cytochrome c. 1. Stopped-flow electron paramagnetic resonance as a probe for protein folding/unfolding of the C-terminal helix spin-labeled at cysteine 102, *Biochemistry 36*, 2884−2897.
37. Kaplan, R. S., Mayor, J. A., Kotaria, R., Walters, D. E., and McHaourab, H. S. (2000) The yeast mitochondrial citrate transport protein: Determination of secondary structure and solvent accessibility of transmembrane domain IV using site-directed spin labeling, *Biochemistry 39*, 9157−9163.
38. Gross, A., and Hubbell, W. L. (2002) Identification of protein side chains near the membrane-aqueous interface: A site-directed spin labeling study of KcsA, *Biochemistry 41*, 1123−1128.
39. Wang, X., Wang, C. S., Tang, J., Dyda, F., and Zhang, X. C. (1997) The crystal structure of bovine bile salt activated lipase: Insights into the bile salt activation mechanism, *Structure 5*, 1209−1218.
40. Donner, J., Spink, C. H., Borgström, B., and Sjöholm, I. (1976) Interactions between pancreatic lipase, colipase and taurodeoxycholate in the absence of triglyceride substrate, *Biochemistry 15*, 5413−5417.
41. Patton, J. S., Albertsson, P. A., Erlanson, C., and Borgström, B. (1978) Binding of porcine pancreatic lipase and colipase in the absence of substrate studied by two-phase partition and affinity chromatography, *J. Biol. Chem. 253*, 4195−4202.
42. Momsen, W. E., and Brockmann, H. L. (1976) Inhibition of pancreatic lipase B activity by taurodeoxycholate and its reversal by colipase, *J. Biol. Chem. 251*, 384−388.
43. Patton, J. S., Donner, J., and Borgström, B. (1978) Lipase-colipase interactions during gel filtration. High and low affinity binding situations, *Biochim. Biophys. Acta 529*, 67−78.
44. Sternby, B., and Erlanson-Albertsson, C. (1982) Measurement of the binding of human colipase to human lipase and lipase substrates, *Biochim. Biophys. Acta 711*, 193−195.
45. Sarda, L., and Desnuelle, P. (1958) Action de la lipase pancréatique sur les esters en emulsion, *Biochim. Biophys. Acta 30*, 513−521.
46. Ferrato, F., Carriere, F., Sarda, L., and Verger, R. (1997) A critical reevaluation of the phenomenon of interfacial activation, *Methods Enzymol. 286*, 327−347.
47. Mingarro, I., Abad, C., and Braco, L. (1995) Interfacial activation-based molecular bioimprinting of lipolytic enzymes, *Proc. Natl. Acad. Sci. U.S.A. 92*, 3308−3312.
48. Gonzalez-Navarro, H., Bano, M. C., and Abad, C. (2001) The closed/open model for lipase activation. Addressing intermediate active forms of fungal enzymes by trapping of conformers in water-restricted environments, *Biochemistry 40*, 3174−3183.

BI0616089